Geomechanics and Engineering, *Vol. 41, No. 1 (2025) 115-127*
https://doi.org/10.12989/gae.2025.41.1.115

Shear strength of crosslinked xanthan gum biopolymer treated sand-clay mixture

Jeong-Uk Bang[1a], Minhyeong Lee[2b], Dong-Yeup Park[1c] and Gye-Chun Cho*[1]

[1]*Department of Civil and Environmental Engineering, Korea Advanced Institute of Science and Technology, 291 Daehak-ro, Yuseong-gu, Daejeon 34141, Republic of Korea*
[2]*Disposal Safety Evaluation Research Division, Korea Atomic Energy Research Institute, 111 Daedeok-daero 989beon-gil, Yuseong-gu, Daejeon 34057, Republic of Korea*

(*Received December 7, 2024, Revised February 24, 2025, Accepted March 10, 2025*)

Abstract. Cr^{3+}-crosslinked xanthan gum (CrXG) has emerged as a promising solution for enhancing moisture resilience, wet strength, and durability in biopolymer-soil treatment (BPST) applications. However, its shear strength behavior across diverse soil compositions remains insufficiently explored. This study investigates the shear strength characteristics of CrXG-soil composites, spanning from poorly graded sand to clayey silty sand using direct shear tests (DST) under varying moisture states (initially wet, dried, and re-submerged). The results show that CrXG treatment achieves optimal performance in pure sand at low confinement, with an increase in cohesion and a decrease in internal friction angle. Adding clay particles accelerates the crosslinking process, with CrXG-soil composite with 15% clay content (CSM_{15}) demonstrating consistent shear strength improvements across all confining stresses due to agglomeration effects of the CrXG-clay matrix. XG-treated composites exhibit significant strength gains when dried but suffer severe strength losses upon re-submersion due to swelling. In contrast, CrXG-treated CSM_{15} retains shear strength across moisture states, demonstrating superior environmental resilience. These findings highlight the potential of CrXG-treated CSM_{15} for sustainable geotechnical applications, including slope stabilization and erosion control.

Keywords: biopolymer soil treatment; direct shear test; gel phase; sand-clay mixture; shear strength; xanthan gum

1. Introduction

With the intensification of extreme climate change, increased precipitation rates and frequency have accelerated unexpected geotechnical engineering hazards (Chang *et al.* 2019, Ma *et al.* 2021). In response, the demand for sustainable ground improvement methods, such as microbiologically induced calcium carbonate precipitation (MICP), enzyme-induced carbonate precipitation (EICP), and biopolymer-based soil treatment (BPST), have emerged as a promising approach (Lu *et al*. 2023; Pratama *et al.* 2024). Markedly, BPST, which uses naturally derived polysaccharides from plants, microorganisms, or fungi, provides an environmentally friendly and cost-effective alternative for soil stabilization, offering a low carbon footprint throughout production and application.

Among biopolymers, Xanthan gum (XG) has been particularly studied for its ease of workability and its effectiveness in enhancing soil engineering properties, forming a highly viscous hydrogel even at low concentrations (Fatehi *et al*. 2021). Previous works have highlighted its benefits in improving dry unconfined compressive strength (UCS) (Chang *et al*. 2015a, Muguda *et al*. 2017), reducing permeability (Bouazza *et al*. 2009, Cabalar *et al*. 2017), increasing erosion resistance (Kwon *et al.* 2020), preventing desertification (Chang *et al*. 2015b, Tran *et al*. 2020), controlling dust (Chen *et al*. 2015), and enhancing durability (Qureshi et al., 2017), and compaction promotion (Latifi *et al*. 2017, Lee *et al*. 2022). Field-scale applications of XG have further demonstrated its effectiveness in enhancing levee slope erosion resistance (Chang *et al*. 2020, Kang *et al*. 2021, Kwon *et al*. 2023).

Alongside promising enhancement on engineering parameters, the shear strength of XG-treated soils was also examined to address the stress-dependent shearing behavior. Works by Cabalar and Canakci (2011) identified the XG ratio as dominant in sandy soils, while Lee *et al.* (2017) demonstrated that even a 1% XG treatment can yield sufficient shear strength—with different gel states exhibiting distinct behaviors. For lean clays, increased XG content tends to enhance cohesion and reduce the friction angle (Cabalar *et al*. 2018), whereas in cohesionless soils, cohesion improves markedly with little change in friction angle (Soldo and Miletić 2019). Additionally, drying conditions and cyclic drying–wetting cycles also influence strength—drying enhances shear strength (Chen *et al*. 2019, Chen *et al*. 2020), although most of these gains are reversed upon re-wetting. Lee *et al*. (2020) and Zhang *et al*. (2024)

*Corresponding author, Professor
E-mail: gyechun@kaist.edu
[a]Graduate student
E-mail: jeonguk.bang@kaist.ac.kr
[b]Senior researcher
E-mail: leemh@kaeri.re.kr
[c]Graduate student
E-mail: dypark2160@kaist.ac.kr

ISSN: 2005-307X (Print), 2092-6219 (Online)

further highlighted that gel moisture state, surface asperity, and curing time play significant roles in the interfacial behavior and overall shear strength during moisture variations. In summary, studies on XG-treated soils consistently show that the XG ratio, base soil type, and water content are key factors influencing shear strength.

However, XG's hydrophilic nature raises concerns about its durability, as re-exposure to moisture can cause significant strength loss (Lee *et al*. 2022). To address this limitations, recent studies have investigated rheological modifications of XG through crosslinking with multivalent cations, such as Na^{+}, Ca^{2+}, and Cr^{3+} (Lee *et al*. 2023a, Lee *et al.* 2023b, Lee *et al*. 2023c). Among these, Cr^{3+}-crosslinked XG (CrXG) has demonstrated rapid enhancement of wet UCS in cohesionless sand while maintaining workability and sustained strength durability against long-term immersion, though its effectiveness diminishes under dehydrated curing conditions. Additionally, incorporating a preferred clay content in CrXG biopolymer-soil composites has been shown to enhance strength durability under accelerated and atmospheric weathering conditions, irrespective of curing environments (Bang *et al.* 2024). Despite these advances, a comprehensive understanding of the interactions between CrXG biopolymer and soils, and particularly their shear strengthening behavior in sand-clay mixtures, remains lacking. Gaining such insights is crucial for optimizing CrXG applications in slope surface protection to mitigate hydraulic and wind erosion effectively.

This study investigates the shear strength parameters of CrXG-treated sand-clay mixtures, focusing on the influence of curing time, clay content, and changes in moisture state under varying environmental conditions. Direct shear tests (DST) are conducted to evaluate the effects of clay content on the shear strength behavior of CrXG-treated soil composites over time, comparing strength evolution across different moisture states (initially wet, dried, and resubmerged) for untreated (UT), XG-treated, and CrXG-treated specimens. Furthermore, microscopic analysis of CrXG-treated specimens is employed to elucidate inter-particle bonding within the soil-binder matrix, providing valuable insights for optimizing CrXG applications in sustainable geotechnical solutions.

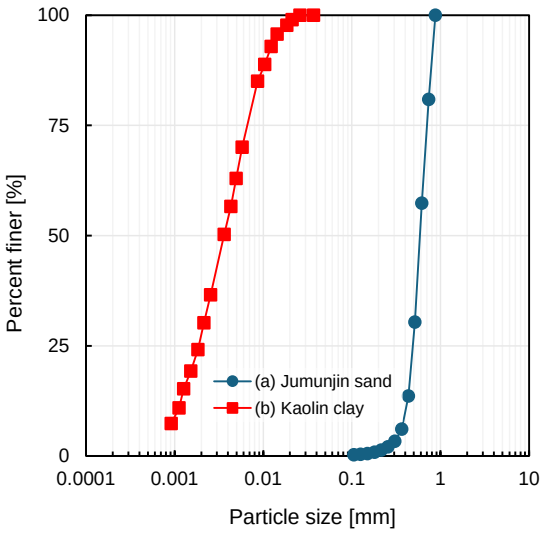

Fig. 1 Particle size distribution curve of Jumunjin sand and kaolin clay

Table 1 Basic soil properties of Jumunjin sand and kaolinite clay

Jumunjin sand	
Specific gravity	2.65
Mean particle size [μm]	507
Coefficient of uniformity	1.94
Coefficient of curvature	1.09
Maximum void ratio	0.89
Minimum void ratio	0.64
USCS	SP
Kaolinite	
Specific gravity	2.65
Mean particle size [μm]	3.7
Liquid limit [%]	70
Plastic limit [%]	24
Plasticity index [%]	46
Specific surface area, SSA [m^2/g]	22
USCS	CH

2. Materials and methods

2.1 Used soil

To examine the effect of fine content in sand-clay mixtures, Jumunjin sand and kaolinite clay were selected as host soils. Jumunjin sand is classified as poorly-graded sand (SP) according to the Unified Soil Classification System (USCS). Its particle size distribution of sand particles is shown in Fig. 1, with a mean particle size (D_{50}) of 507 μm. X-ray diffraction (XRD) analysis indicates that sand primarily comprises 72% quartz, 22% microcline, and 6% albite.

The kaolinite clay, sourced from Belitung Island, Indonesia, has is D_{50} of 3.7 μm classified as highly plastic clay (CH) according to the USCS. Composed mostly of kaolinite (89%) and a minor fraction of illite (11%), this kaolinite has plastic and liquid limits of 24% and 70%, respectively. Detailed soil properties are summarized in Table 1.

2.2 Biopolymers

Xanthan gum (XG) is an ionic polysaccharide biopolymer produced by *Xanthomonas campestris*. Its 1,4-linked β-D-glucose backbone features anionic trisaccharide side chains, which readily attract water molecules to form a three-dimensional hydrophilic hydrogel network (Casas *et al.* 2000, Peppas 1986). This hydrogel exhibits swelling

Table 2 Details of soil composition of sand-clay mixtures

Label	Composition [%]		G_s	D_{10}	OMC	γ_{dmax}
	Sand	Clay	[-]	[mm]	[%]	[g/cm^3]
CSM_0	100	0	2.623	0.4012	11.1	15.55
CSM_{15}	85	15	2.623	0.0081	13.0	17.72
CSM_{30}	70	30	2.629	0.0011	14.0	17.93

* G_s: specific gravity; D_{10}: effective diameter; OMC: optimum moisture content; γ_{dmax}: maximum dry unit weight

and viscous characteristics, enhancing soil stabilization through interparticle coating, bridging, and pore-filling mechanisms (Chang *et al*. 2015a).

When cross-linked with Cr^{3+} cations, XG transitions into a rigid hydrogel (CrXG) with increased intermolecular connectivity. This cross-linking induces hydrophobic behavior, preventing reactivation under immersed conditions (Bueno *et al.* 2013). In this study, research-grade XG powder (CAS No. 11138–66-2; Merck, USA) and chromium nitrate nonahydrate ($Cr(NO_3)_3 \cdot 9H_2O$, CAS: 778902-08; Daejung Chemical Co., Korea) were used. Sodium chloride (NaCl) was included to enhance the binding between XG and Cr^{3+} by mitigating repulsive forces (Pelletier *et al*. 2001, Rochefort and Middleman 1987).

2.3 Specimen preparation

Three sand-clay mixtures (CSMs) were prepared with kaolinite mass fractions of 0%, 15%, and 30%, denoted as CSM_0, CSM_{15}, and CSM_{30}, respectively. Jumunjin sand and kaolinite clay were oven-dried, mixed at the desired ratios, and classified under the USCS as poorly-graded sand (SP) for CSM_0 and silty and clayey sand (SC-SM) for CSM_{15} and CSM_{30}. Detailed soil properties of the CSMs are detailed in Table 2.

Specimens were categorized into three treatment types: untreated (UT), XG-treated, and CrXG-treated. UT specimens were dry-mixed at the given sand-to-clay ratio, adjusted to an initial water content of 20%, and compacted directly into shear box molds (60 mm diameter × 20 mm height) with dry unit weight of 1.58 ± 0.08 g/cm³. For biopolymer treatments, both XG and CrXG were prepared with a fixed XG-to-soil mass ratio of 1% and an initial water content of 20%, following previous studies that identified these conditions as optimal for achieving effective mixing workability and strength performance (Cabalar and Canakci 2011, Fatehi *et al.* 2023, Seo *et al*. 2021, Vydehi *et al*. 2022).

For XG-treated soil specimens, the hydrogel was prepared by dissolving powdered XG in deionized water at an XG-to-water mass ratio (m_x/m_w) of 5%. The prepared XG hydrogel was thoroughly mixed with the CSMs and then either molded into specimen rings or directly into the shear box, depending on the experimental requirements. Since XG-treated soils do not exhibit progressive strengthening over time under constant water content, specimens were molded at the target density directly in the shear box and tested immediately after molding; alternatively, air-dried specimens were cast in cylindrical molds and naturally cured for 28 days prior to testing. For resubmerged conditions, air-dried cylindrical XG specimens were placed in the shear box and submerged in deionized water for 24 hours before direct shear testing to account for the hydrophilic behavior of XG.

For CrXG treatment, an aqueous Cr^{3+} solution (comprising 30% $Cr(NO_3)_3 \cdot 9H_2O$ and 10% NaCl by XG mass) was blended with the XG hydrogel at a final ratio of 10:3:1 (XG:$Cr(NO_3)_3$:NaCl) to facilitate crosslinking (Lee *et al*. 2023c). The resulting CrXG hydrogel was thoroughly mixed with the CSMs, molded into cylindrical molds, and cured in a sealed container to prevent moisture loss during curing. It should be noted that in this study “wet curing” refers to maintaining the target water content without submerging the specimens, and without drying, as CrXG-treated soils develop via Cr^{3+}-XG gelation. After 28 days, the specimens were air-dried for an additional 28 days to prepare for testing under 'dried' conditions. Finally, the dried samples were submerged in deionized water to evaluate their performance under the “resubmerged” state, as CrXG-treated specimens demonstrated self-standing durability when saturated. The detailed experimental procedures and conditions are summarized in Table 3.

2.4 Direct shear test

Direct shear (DS) tests were performed to evaluate the shear behavior and strength of biopolymer-treated soil specimens. The experiments utilized a laboratory direct shear testing machine (HM-5750D.3F, Humboldt Mfg. Co.), equipped with a shear load frame and LVDTs for precise measurement of vertical and horizontal strains. Vertical confining stresses (σ_{vc}) of 50, 100, 200, and 400 kPa were applied until the specimens reached a constant vertical strain. Shear loading was conducted in accordance with ASTM D3080 (ASTM, 2023) standards, using a constant horizontal displacement rate of 0.6 mm/min (equivalent to 1% strain per minute) until a maximum horizontal strain of 15% was achieved. For each testing condition, three replicate tests were conducted, and the average values of peak and residual shear strengths were reported.

2.5 Microscopic observation via scanning electron microscopy

To investigate the microstructure and evaluate the effect of CrXG treatment at varying clay contents, scanning electron microscopy (SEM) analysis was performed.

Table 3 Experimental program in this study

Test	Base soil type	Treatment	Curing condition	Curing time [day]	Confining stress [kpa]
DST	CSM_0, CSM_{15}, CSM_{30}	Untreated	Initial state		50, 100, 200, 400
	CSM_0, CSM_{15}, CSM_{30}	CrXG 1%	Initial state ↓ Wet curing state ↓ Air dried state ↓ Resubmerged	0, 1, 4, 7, 14, 28 28 1	
	CSM_0, CSM_{15}, CSM_{30}	XG 1%	Initial state ↓ Air dried state ↓ Resubmerged	 28 1	
SEM	CSM_0, CSM_{15}, CSM_{30}	CrXG 1%	Air dried state	28	-

Images were captured using a JSM-IT800 Field Emission SEM (Jeol Ltd., Japan). CrXG-treated specimens dried for 28 days were fixed onto the specimen mount using carbon conductive adhesive. To prevent surface electron charging and enhance image resolution, the specimens were coated with a platinum sputtering layer.

3. Results and discussion

3.1 Effect of curing conditions and soil compositions on direct shear strength behavior of CrXG-treated soil

In this section, the effects of curing time and clay content on the shear behavior of CrXG-treated CSMs were evaluated. Fig. 2 presents the shear stress and vertical strain responses versus horizontal strain for UT and CrXG-treated soil specimens. For CSM_0 at σ_{vc} = 50 kPa, the peak shear strength (τ_f) progressively increases with curing time, consistent with findings by Lee *et al*. (2023c) (Fig. 2(a)). While UT specimens show strain-hardening behavior without a distinct peak, the CrXG-treated specimens display brittle peak characterized by reduced peak strain (ε_f) and increased residual stress (τ_r) over time. The enhanced τ_f and τ_r observed in CrXG-treated specimens are primarily attributed to the stiffening CrXG gels, which form particle-bridging and coating layers within sand matrix (Lee *et al.* 2023c). This shear strengthening effect is further corroborated by the vertical strain responses. At σ_{vc} = 50 kPa, CrXG-treated specimens showed a pronounced dilation that surpasses the response of UT specimens (Fig. 2(d)). The increased dilatancy indicates that the agglomeration of sand particles by rigid CrXG gel clusters increases resistance within the sand matrix to dilate, contributing to improved shear strength. However, at σ_{vc} = 400 kPa, 1-day-cured CrXG specimens exhibit lower τ_f and τ_r compared to UT specimens. This behavior is attributed to high swelling capacity of freshly formed CrXG gels, which reduce interlocking by hinder consolidation at vertical loading stage (Babatunde *et al.* 2023, Judge *et al.* 2022). While gel stiffening occurs with extended curing, both τ_f and τ_r remain lower than those of UT specimens. These findings suggest that the strengthening impact of cured CrXG gels is more pronounced at lower σ_{vc} levels, whereas confinement effects dominate over gelation-induced strengthening at higher σ_{vc} levels.

The addition of clay significantly influences the gelation dynamics in XG-Cr^{3+} gels, altering the shear strength characteristics of CrXG-treated specimens. For both CSM_{15} and CSM_{30}, a notable increase in τ_f is observed at σ_{vc} = 50 kPa, while τ_r shows minimal variation (Figs. 2(b) and 2(c)). However, the differences in strength between specimens cured for 1, 7 and 28 days are less pronounced compared to CSM_0, suggesting an earlier completion of the gelation process. The clay particles likely interfere with the crosslinking reactions between XG polymers and Cr^{3+} ions, restricting further gelation and leading to reduced stiffening over time (Garver *et al.* 1989).

At σ_{vc} = 400 kPa, τ_f and τ_r show noticeable improvement in CSM_{15}, while no significant changes are evident in CSM_{30}. As reported by Chang and Cho (2018), the inclusion of clay particles in biopolymer matrices induces a conglomeration effect, effectively creating secondary particles. This behavior enhances particle interlocking, contributing to increased shear strength and dilation in CSM_{15}. Conversely, in CSM_{30} with higher clay content, the impact of CrXG treatment on τ_f and τ_r is negligible across curing times, and vertical strain remains largely unchanged (Fig. 2(f)). These findings support the hypothesis that increasing clay content further impedes XG-Cr^{3+} crosslinking, thereby reducing the effectiveness of gelation (Bang et al., 2024).

Fig. 3 presents the direct shear strengths of UT, XG, and CrXG-treated CSMs, where the experimental data were fitted using the Mohr-Coulomb failure line. The derived cohesion (c_d) and friction angle (ϕ_d) are shown in Fig. 4, which illustrates the evolution of shear strength parameters with curing time. Overall, direct shear strength exhibits a linear increase with overburden stress across all soil compositions and biopolymer treatments. For CSM_0 (Fig. 3(a)), the Mohr-Coulomb (MC) failure envelopes for UT, XG, and 1-day cured CrXG-treated specimens show minimal

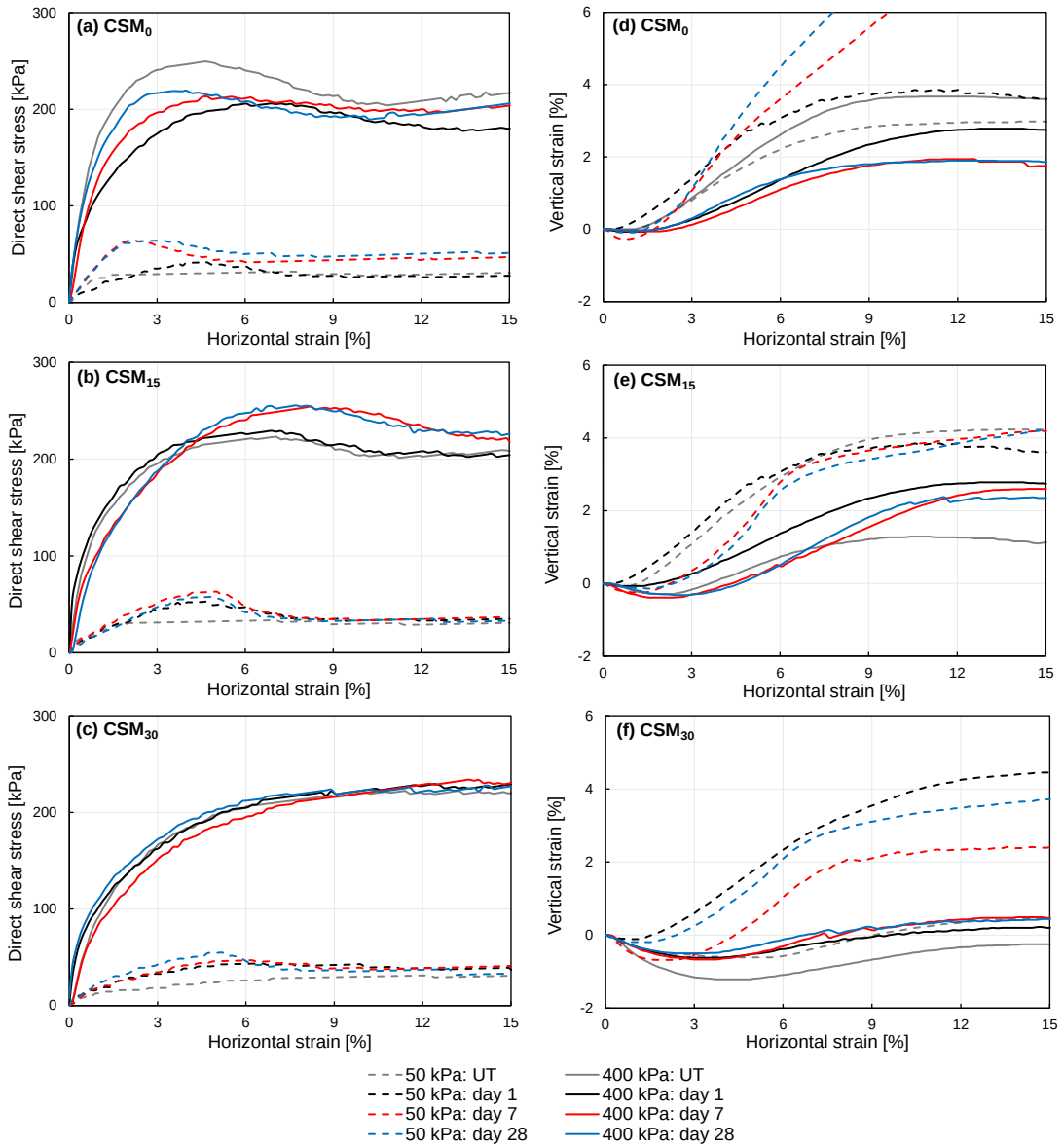

Fig. 2 Direct shear test results for UT and CrXG-treated CSMs at different curing times: (a)-(c) direct shear stress vs. horizontal strain relationship; (d)-(f) vertical strain vs. horizontal strain relationship

differences initially. However, time-dependent strength development in CrXG-treated specimens shifts the failure envelope upward, with cohesion (c_d) increasing significantly up to 14 days of curing (Fig. 4(a)). A notable observation is the contrasting effects of CrXG treatment depending on confinement levels. At low confinement ($\sigma_{vc} \leq 100$ kPa), CrXG treatment shows a higher improvement efficiency, increasing cohesion from nearly zero to over 44 kPa after 28 days of curing.

Conversely, at higher confinement ($\sigma_{vc} \geq 200$ kPa), CrXG-treated specimens exhibit smaller τ_f values compared to UT specimens, despite slight time-dependent stiffening in the CrXG hydrogel. These results align with previous findings indicating that the cementation effect of CrXG gel diminishes as vertical confinement increases (Lee *et al.* 2023b). This behavior can be attributed to the compressibility of CrXG hydrogel within the sand matrix, which affects interlocking mechanisms at higher σ_{vc}.

Fig. 5 shows the initial vertical strain (before shearing) under confinement for UT and CrXG-treated CSMs. At low σ_{vc}, CrXG-treated CSM_0 exhibits lower initial settlement compared to UT specimens (denoted by the hatched area). As curing progresses, the initial vertical strain diminishes in both low and high σ_{vc}, indicating that the stiffer CrXG gel resists compression more effectively than UT specimens. This increased stiffness, however, reduces shear strength, which is primarily driven by interparticle friction under high σ_{vc} conditions. Ultimately, this behavior results in a reduction of internal friction angle (ϕ_d) of CrXG-treated CSM_0 from 32° to 24° (Fig. 4(b)), highlighting the reduced efficiency of CrXG treatment under high confinement conditions

CrXG treated CSM_{15} exhibited gradual strength development across all stress ranges, characterized by an increase in cohesion (c_d) while maintaining a constant internal friction angle (ϕ_d). The improvement across all σ_{vc}

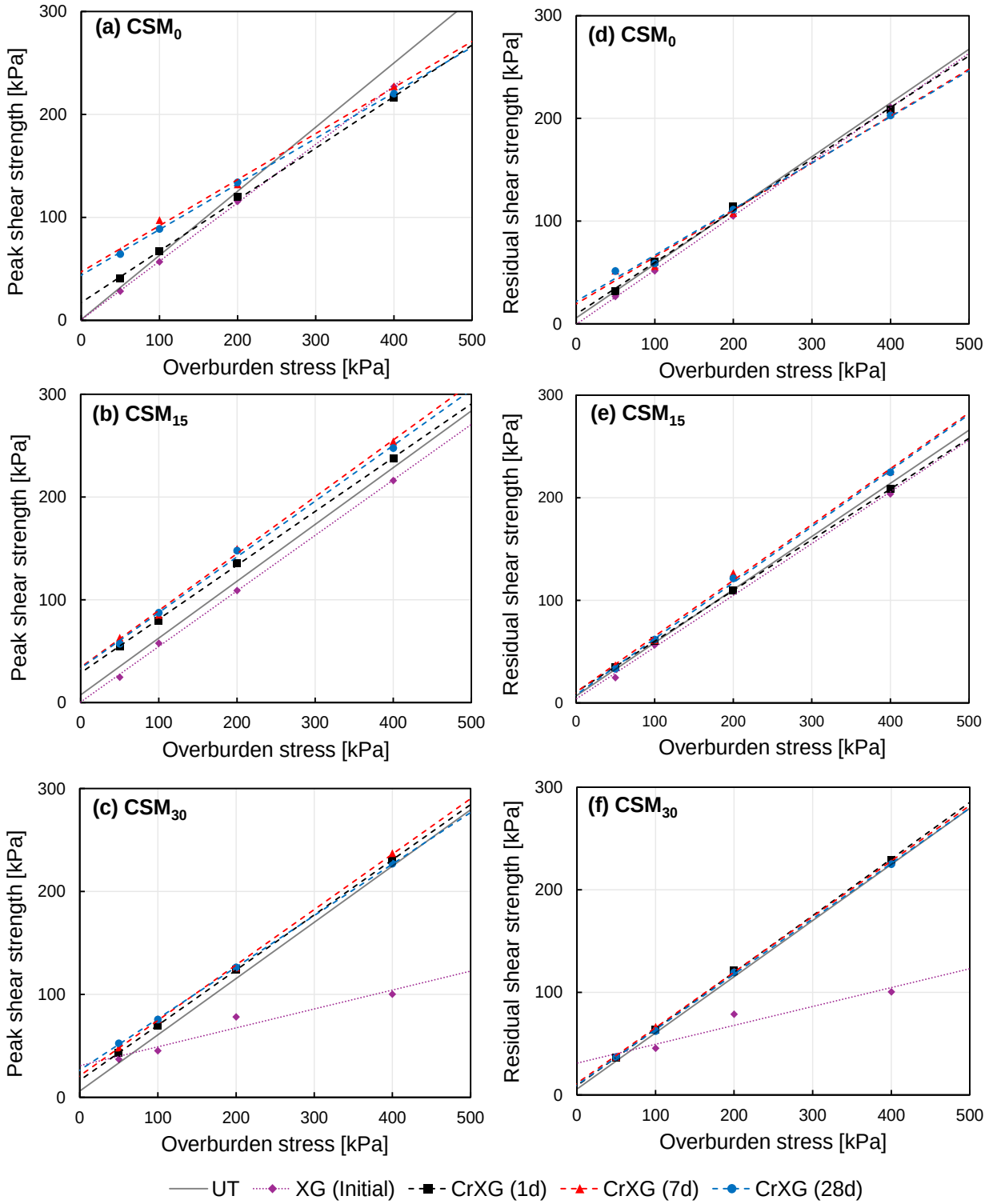

Fig. 3 Relationships between peak and residual direct shear strength (τ_f and τ_r) and overburden stress (σ_{vc}) for UT, XG, and CrXG treated specimens. Mohr–Coulomb failure lines are shown: solid lines indicate UT-, dotted lines indicate XG-, and dashed lines indicate CrXG-treated specimens. (a), (d) CSM_0; (b), (e) CSM_{15}; and (c), (f) CSM_{30}

levels resulted in c_d increasing from 9 to 34 kPa, with most strength development casing within 4 to 7 days of curing (Fig. 4(a)). This early completion of gelation compared to CSM_0 suggests that the CrXG-clay matrix forms a stiffer structure than pure CrXG gel, inducing greater shear resistance even under higher σ_{vc}. In contrast, XG treated CSM_{15} displayed reduced shear strength across all σ_{vc} ranges (Fig. 3(b)). This decrease aligns with previous studies, which hypothesize that repulsive forces between XG and clay particles disrupt inter-particle bonding, ultimately weakening the shear strength (Cabalar *et al.* 2018, Nugent 2011).

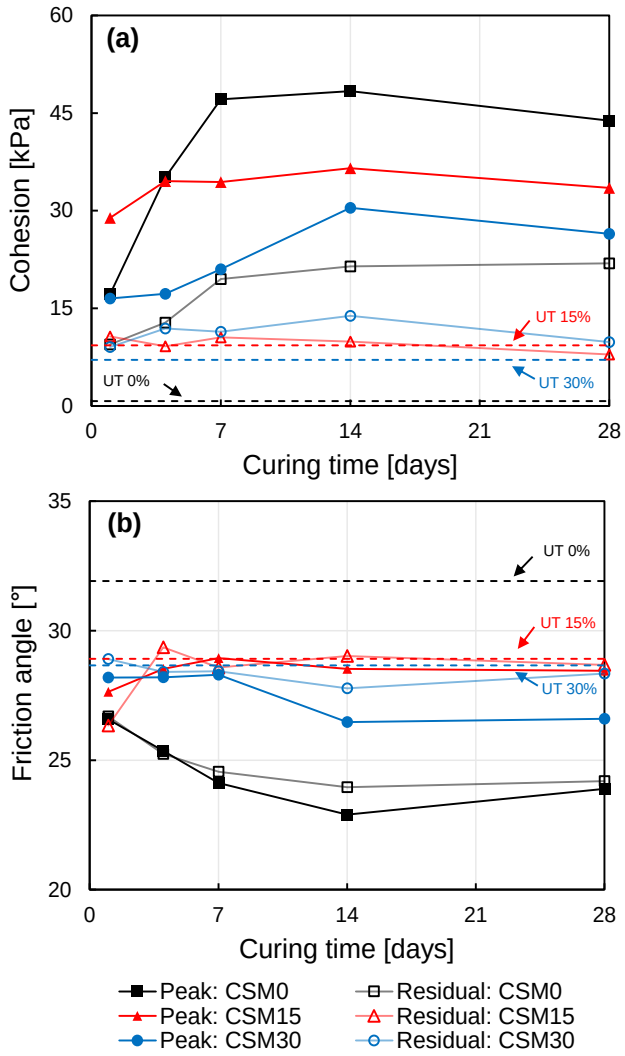

Fig. 4 Peak and residual shear strength parameters variations by curing time. (a) cohesion (c_d), and (b) internal friction angle (ϕ_d)

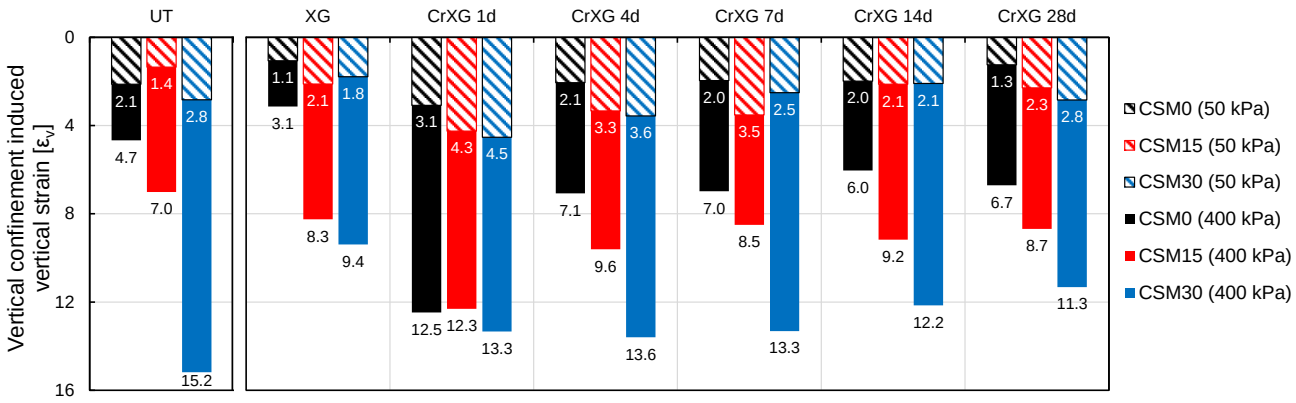

Fig. 5 Time dependent initial vertical strain under vertical confinement of UT and CrXG treated specimens

For CSM_{30}, the effects of XG and CrXG treatments on shear strengths were markedly different. CrXG-treated specimens exhibited slight improvements in shear strength, showing increased c_d and a small reduction in ϕ_d, a behavior consistent with CSM_0. In contrast, XG-treated specimens experienced significant reductions in shear strength, particularly at $\sigma_{vc} > 100$ kPa, where ϕ_d dropped drastically from 28.7° to 10.4° (Fig 3c). This decline is attributed to the combined effects of XG-clay particle repulsion and the high swelling characteristics of both the XG hydrogel and clay matrix, which become more pronounced with increased clay content. Residual shear strength showed distinct trends

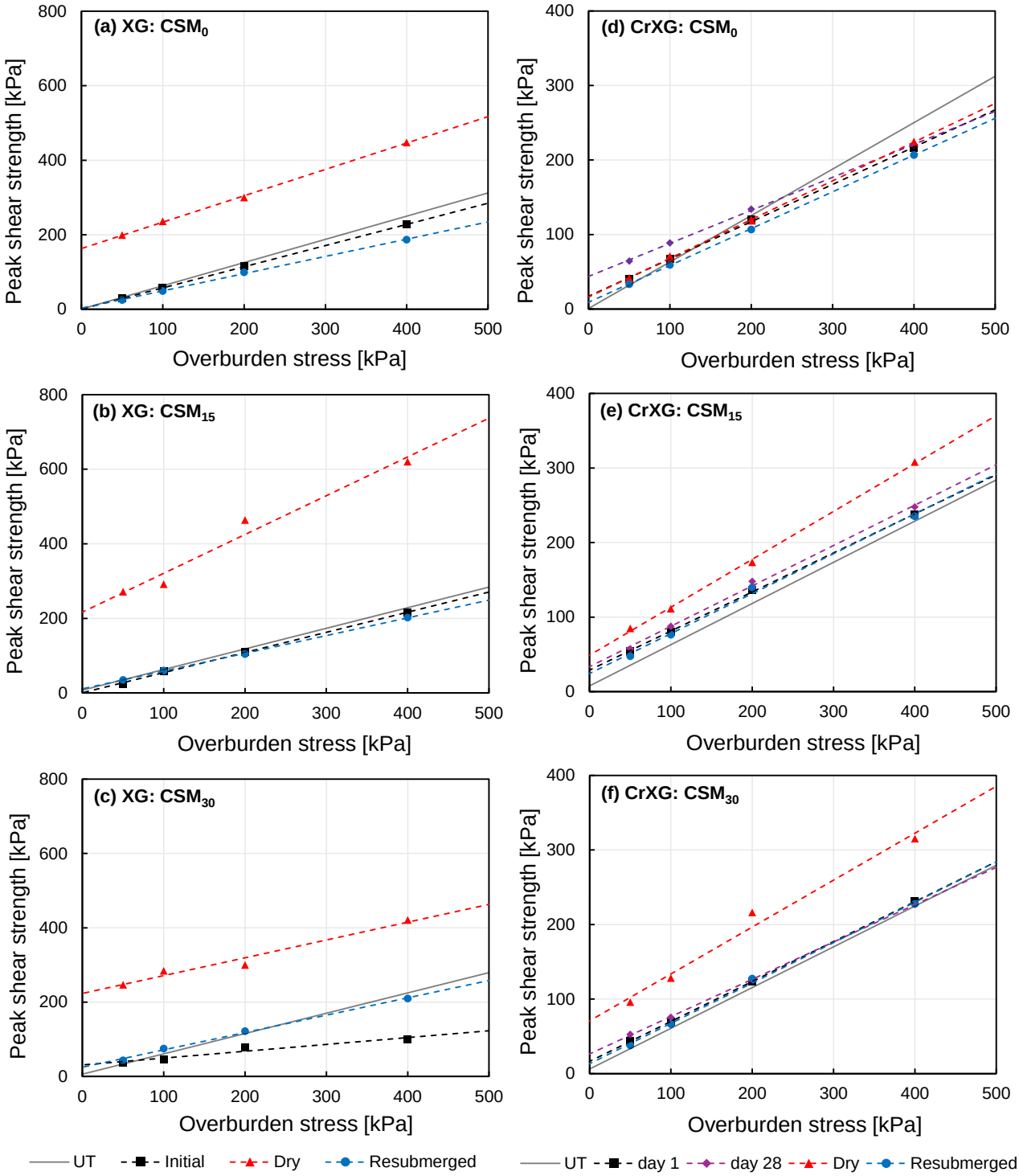

Fig. 6 Peak direct shear strength-overburden stress of XG treated specimens under gel state variation; (a) CSM_0; (b) CSM_{15}; and (c) CSM_{30}; Peak direct shear strength-overburden stress of CrXG treated specimens under gel state variation; (d) CSM_0; (e) CSM_{15}; and (f) CSM_{30}

depending on the presence of clay particles (Figs. 3(d)-3(f) and Fig. 4**).** In CSM_0, CrXG treatment maintained approximately 50% of the c_d while retaining a constant ϕ_d, whereas CSM_{15} and CSM_{30} lost most of the improvements in both c_d and ϕ_d post-shearing. This marginal change in residual shear strength is likely due to the fragmentation of CrXG gel into smaller particles at large strains, rendering the gel's contribution negligible (Lee *et al*. 2017).

3.2 Shear strength evolution in XG- and CrXG-treated CSMs across different moisture states

This section introduces the evolution of shear strength across different moisture states (initially wet, dried, and resubmerged) in XG and CrXG-treated CSMs. Fig. 6 illustrates the relationship between peak shear stress and overburden stress for XG and CrXG-treated specimens

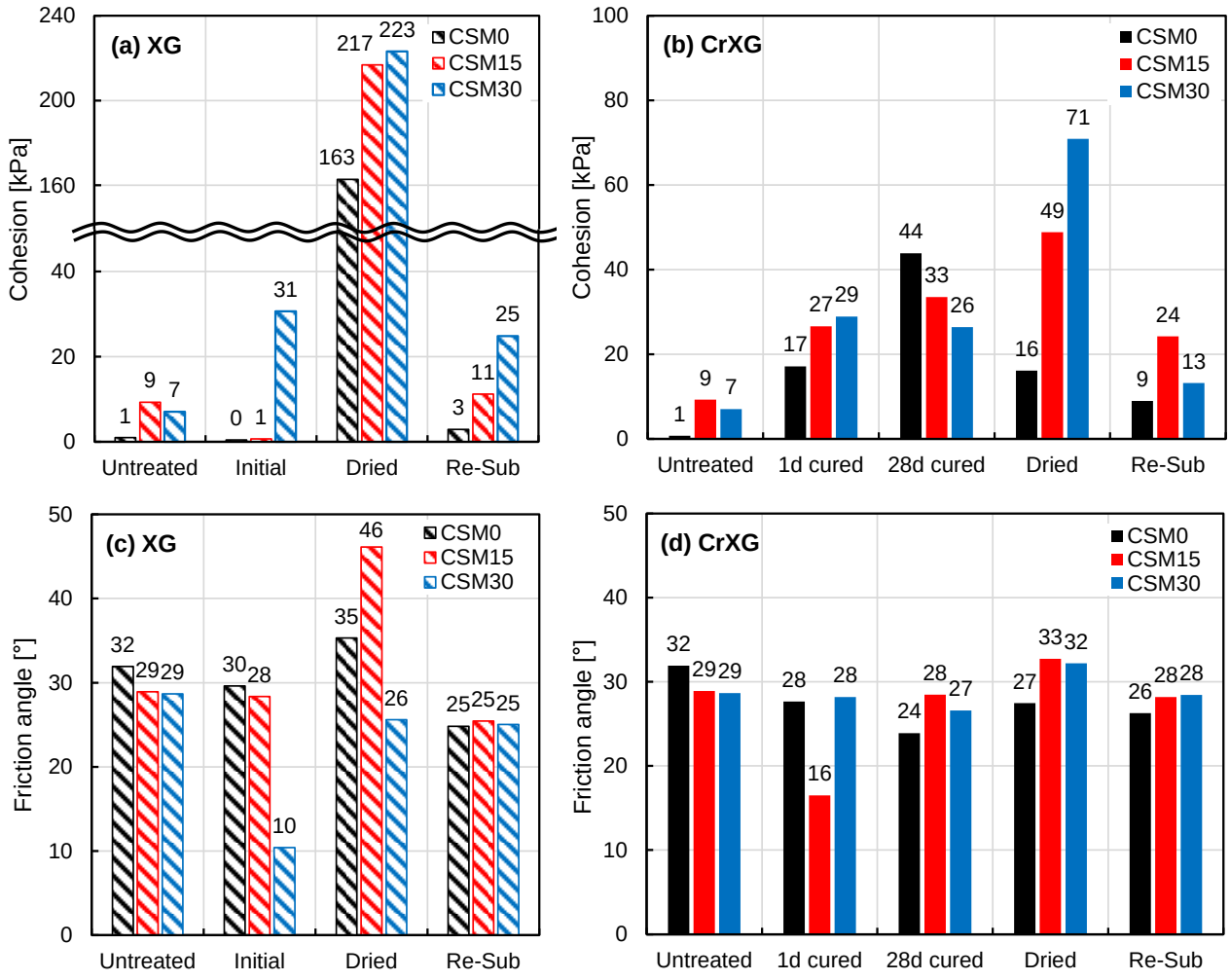

Fig. 7 Peak shear strength parameters of XG- and CrXG-treated CSMs depending on moisture state; (a and b) cohesion (c_d), and (c and d) internal friction angle (ϕ_d)

under varying moisture states. Fig. 7 presents the corresponding peak shear strength parameters from Mohr-Coulomb failure line, with detailed results summarized in Tables 4 and 5, respectively.

XG-treated CSMs exhibit significant variations in shear strength across different moisture states due to the transformation of XG from a viscous hydrogel to a plastic solid and ultimately to a dissolved state (Figs. 6(a)-6(c)). The initial low shear strength of XG-treated specimens compared to UT specimens is attributed to the repulsive interactions between XG and clay particles, which disrupt inter-particle bonding and weaken shear resistance due to the viscous nature of the XG hydrogel (Cabalar *et al.* 2018, Nugent 2011). Upon drying for 28 days, shear strength increases notably as the condensed XG-clay matrix cements coarse particles, resulting in enhanced cd values of 163, 217, and 223 kPa for CSM_0, CSM_{15}, and CSM_{30}, respectively (Fig. 7(a)). This improvement effect is more pronounced in the presence of clay particles, owing to direct ionic bonding between XG side chains and electrically charged clay particles (Cabalar and Canakci 2011, Chang *et al*. 2015a, Chen *et al.* 2019). However, when XG-treated CSMs are re-exposed to water, shear strength diminishes drastically. For instance, XG-treated CSM_0 shows a dramatic reduction in c_d from 163 kPa to 3 kPa after re-submersion. This water susceptibility has also been demonstrated through cyclic wetting-drying tests, where XG-treated sand-clay mixtures lost their unconfined compressive strength after repeated cycles (Lee *et al*. 2022, Soldo and Miletic 2022) This strength degradation results from the dissolution and swelling of the hydrophilic XG hydrogel, which weakens the matrix structure. In the presence of water, the functional groups or side chains of XG molecules are reactivated, causing the swollen XG hydrogel to lose particle bridging capacity and act as a lubricant, promoting particle sliding (Lee *et al*. 2017). Although some c_d is retained in CSM_{15} and CSM_{30} due to hydrogen bonding with clay particles, the internal friction angle (ϕ_d) decreases across all compositions (e.g., from 29° to 25° for CSM_{30}) (Fig. 7(b)). These comparable ϕ_d values, regardless of soil composition, imply the dominant role of the swollen XG-clay matrix in hindering interparticle friction during shear loading.

CrXG-treated CSM_0 (Figs. 6(d)-6(f)) exhibited contrasting shear strength behavior across different moisture states. For CSM_0, the time-dependent curing effect

Table 4 Peak and residual shear strength parameters of XG treated specimens

		Peak behavior						Residual behavior					
		c_d (KPa)			ϕ_d (KPa)			c_d (KPa)			ϕ_d (KPa)		
		CSM_0	CSM_{15}	CSM_{30}	CSM_0	CSM_{15}	CSM_{30}	CSM_0	CSM_{15}	CSM_{30}	CSM_0	CSM_{15}	CSM_{30}
Untreated		0.7	9.3	7.1	31.9	28.9	28.7	5.8	8.8	6.9	27.6	27.4	28.7
Wet Curing	1 d	17.1	28.9	16.5	26.6	27.6	28.2	9.5	10.7	9.0	26.7	26.3	28.9
	4 d	35.1	34.5	17.2	25.4	28.5	28.2	12.8	9.2	11.9	25.2	29.4	28.4
	7 d	47.1	34.4	21.0	24.1	28.9	28.3	19.5	10.5	11.4	24.6	28.6	28.4
	14 d	48.4	36.5	30.5	22.9	28.5	26.5	21.4	9.9	13.9	24.0	29.0	27.8
	28 d	43.8	33.5	26.4	23.9	28.5	26.6	21.9	7.9	9.8	24.2	28.7	28.3
Dried (28 d)		16.1	48.8	70.9	27.5	32.7	32.2	6.6	7.2	5.8	26.5	30.4	33.9
Resubmerged (1d)		9.0	24.2	13.2	26.3	28.2	28.4	5.1	9.0	5.7	26.5	28.0	29.2

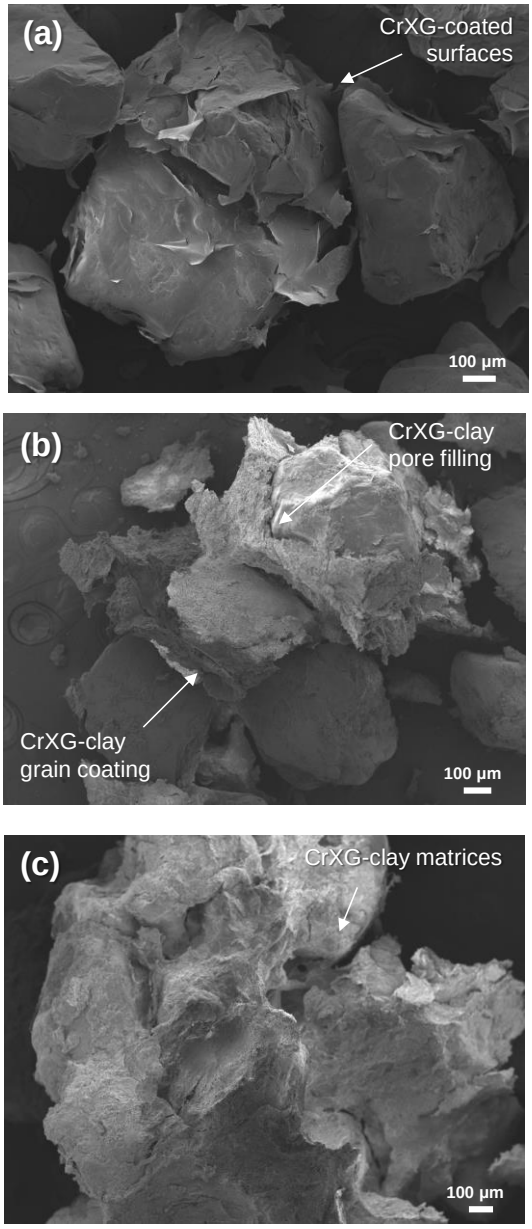

Fig. 8 SEM images of 28 days dried CrXG specimens; (a) CSM_0, (b) CSM_{15}, and (c) CSM_{30}

was noted, exhibiting c_d increases from 1 kPa to 17 and 44 kPa after 1 day and 28 days curing, respectively. Unlike that shear strength enhancement in XG-treated CSM_0, shear strength diminishes upon drying and consequent re-submergence. As reported in Lee *et al.* (2023a), crosslinked polymer tends to be characterized by irreversible volumetric shrinkage upon drying due to less water affinity, resulting fissure and loss of interparticle connection in sand matrix, as also observed in SEM images (Fig. 8(a)). Moreover, water absorption of residual polymer chains induces partial gel softening after re-submergence (Chang *et al*. 2016, Lee *et al.* 2023c).

In the presence of clay particles (Figs. 7(b) and 7(d)), the formation of CrXG-clay matrices within sand particles significantly alters the shear strength behavior of CSM_{15} and CSM_{30} under varying moisture states. With the inclusion of clay, both c_d and ϕ_d increase for dried CrXG-treated CSM_{15} (c_d = 49 kPa) and CSM_{30} (c_d = 71 kPa), surpassing CrXG-treated CSM_0. This improvement is attributed to the transformation of a thin CrXG gel layer around sand grains (Fig. 8(a)) into a CrXG-clay matrix that effectively agglomerates sand particles (Figs. 8(b) and 8(c)). Although the improvement efficiencies for dried CrXG-treated CSMs were lower than those of XG-treated CSMs (c_d > 200 kPa), it is notable that CrXG-treated CSM_{15} and CSM_{30} sustain higher shear strength than both UT and XG-treated CSMs after submergence. Among the CrXG-treated specimens, CSM_{15} exhibits minimal strength reduction upon rehydration compared to CSM_{30}. This behavior is attributed to the competitive intermolecular bonding between Cr^{3+} and clay particles in CSM_{30}, which leaves free clay particles unbound to XG or Cr^{3+}. These unbound particles contribute to additional swelling, leading to a sharp decrease in c_d for CSM_{30}.

In summary, while CrXG-treated CSM_0 exhibits superior wet-state shear strength and XG-treated CSM_{30} demonstrates the highest dry strength, CrXG-treated CSM_{15} emerges as the optimal mixture in terms of shear strength sustainability. The relatively stable performance of CrXG-treated CSM_{15} has been validated through cyclic wetting-drying durability tests, retaining over 90% of unconfined compressive strength after eight cycles (Bang *et al*. 2024).

These findings suggest that incorporating 15% clay content forms a CrXG-clay matrix that provides stable and competitive strength retention under weathering conditions, highlighting its potential for geotechnical engineering applications.

4. Conclusions

This study investigated the evolution of shear strength in XG- and CrXG-treated biopolymer-soil composites with varying fine contents (0–30%) and moisture state changes (initially wet, dried, and re-submerged). Direct shear tests and microscopic imaging were conducted to elucidate the underlying shear strength behaviors and parameters. The key findings are summarized as follows:

- The shear strength of CrXG-treated soil composites is influenced not only by soil composition and curing time but also by confining stress levels. In pure sand (CSM_0), CrXG treatment enhances shear strength at low confinement (50 kPa) but reduces it at high confinement (σ_{vc} over 200 kPa) compared to UT specimens. This behavior results from the rigid CrXG gel's ability to prevent particle deformation through mechanical bonding, while its reduced compressibility mitigates interlocking-induced friction resistance, leading to an increase in c_d and a decrease in ϕ_d.
- Adding clay particles accelerates the completion of CrXG crosslinking, resulting in less significant shear strength variation over curing time. CrXG-treated CSM_{15} demonstrated effective shear strength enhancement across all confining stress levels, attributed to the agglomeration effects of the CrXG-clay matrix between sand particles. In contrast, excessive clay content in CSM_{30} resulted in minor shear strength improvements under both low and high confinement due to inhibited crosslinking efficiency.
- XG-treated CSMs exhibit significant shear strength variations across moisture states. Upon drying, XG-treated CSMs showed marked increases in c_d and ϕ_d, but most of their shear strength was lost when re-submerged, due to the reactivation of XG polymers. CrXG-treated CSMs, particularly those containing clay particles, retained shear strength after drying and rewetting. Notably, CrXG-treated CSM_{15} preserved strength across all conditions, demonstrating that 15% fine content represents an optimal composition for achieving both shear strength and durability under varying environmental conditions.

While this study focused on specific fine contents and moisture states, the findings elucidate the shear strength behavior and parameters of CrXG-treated sand-clay mixtures under diverse conditions expected in geotechnical applications. Among the composites tested, CrXG-treated CSM_{15} demonstrated superior shear strength sustainability, highlighting its potential for geotechnical engineering applications, particularly in scenarios involving atmospheric drying and wetting cycles. Future studies are recommended to expand the applicability of CrXG treatment by exploring particle size distributions, soil grading conditions, and natural soil compositions to enhance its practicality in field applications.

Acknowledgments

This work was supported by the National Research Foundation of Korea (NRF) grant funded by the Korea government (MSIT) (2023R1A2C300559611) and Ministry of Oceans and Fisheries (MOF) of the Korean Government (No. 20220364).

References

ASTM. (2023), ASTM D3080M-23 Standard test method for direct shear test of soils under consolidated drained conditions. *D3080/D3080M*, **3**(9).

Babatunde, Q.O., Yoon, H.K. and Byun, Y.H. (2023), "Rheological behavior of zein biopolymer and stiffness characteristic of biopolymer treated soil", *Constr. Build. Mater.*, **384**, 131466. https://doi.org/10.1016/j.conbuildmat.2023.131466.

Bang, J.U., Lee, M., Park, D.Y., Chang, I. and Cho, G.C. (2024), "Effects of soil composition and curing conditions on the strength and durability of Cr3+-crosslinked biopolymer-soil composites", *Constr. Build. Mater.*, **449**, 138440. https://doi.org/10.1016/j.conbuildmat.2024.138440.

Bouazza, A., Gates, W.P. and Ranjith, P.G. (2009), "Hydraulic conductivity of biopolymer-treated silty sand", *Géotechnique*, **59**(1), 71-72. https://doi.org/10.1680/geot.2007.00137.

Bueno, V.B., Bentini, R., Catalani, L.H. and Petri, D.F.S. (2013), "Synthesis and swelling behavior of xanthan-based hydrogels", *Carbohyd. Polym.*, **92**(2), 1091-1099. https://doi.org/10.1016/j.carbpol.2012.10.062.

Cabalar, A., Wiszniewski, M. and Skutnik, Z. (2017), "Effects of xanthan gum biopolymer on the permeability, odometer, unconfined compressive and triaxial shear behavior of a sand", *Soil Mech. Found. Eng.*, **54**, 356-361. https://doi.org/10.1007/s11204-017-9481-1.

Cabalar, A.F., Awraheem, M.H. and Khalaf, M.M. (2018), "Geotechnical properties of a low-plasticity clay with biopolymer", *J. Mater. Civil. Eng.*, **30**(8), 04018170. https://doi.org/10.1061/(ASCE)MT.19435533.0002380.

Cabalar, A.F. and Canakci, H. (2011), "Direct shear tests on sand treated with xanthan gum", *Proc Inst Civ Eng Ground Improv*, **164**(2), 57-64. https://doi.org/https://doi.org/10.1680/grim.800041

Casas, J.A., Santos, V.E. and García-Ochoa, F. (2000), "Xanthan gum production under several operational conditions: Molecular structure and rheological properties", *Enzyme Microb. Technol.*, **26**(2-4), 282-291. https://doi.org/10.1016/S0141-0229(99)00160-X.

Chang, I., Im, J. and Cho, G.C. (2016), "Geotechnical engineering behaviors of gellan gum biopolymer treated sand", *Can. Geotech. J.*, **53**(10), 1658-1670. https://doi.org/10.1139/cgj-2015-0475.

Chang, I., Im, J., Prasidhi, A.K. and Cho, G.C. (2015a), "Effects of xanthan gum biopolymer on soil strengthening", *Constr. Build. Mater.*, **74**, 65-72. https://doi.org/10.1016/j.conbuildmat.2014.10.026.

Chang, I., Lee, M. and Cho, G.C. (2019), "Global CO2 emission-related geotechnical engineering hazards and the mission for sustainable geotechnical engineering", *Energies*, **12**(13). https://doi.org/10.3390/en12132567.

Chang, I., Lee, M., Tran, A.T.P., Lee, S., Kwon, Y.M., Im, J. and Cho, G.C. (2020), "Review on biopolymer-based soil treatment (BPST) technology in geotechnical engineering practices", *Transport. Geotech.*, 24. https://doi.org/10.1016/j.trgeo.2020.100385.

Chang, I., Prasidhi, A.K., Im, J., Shin, H.D. and Cho, G.C. (2015b), "Soil treatment using microbial biopolymers for anti-desertification purposes", *Geoderma*, **253-254**, 39-47. https://doi.org/10.1016/j.geoderma.2015.04.006.

Chen, C., Wu, L., Perdjon, M., Huang, X. and Peng, Y. (2019), "The drying effect on xanthan gum biopolymer treated sandy soil shear strength", *Constr. Build. Mater.*, **197**, 271-279. https://doi.org/10.1016/j.conbuildmat.2018.11.120.

Chen, R., Lee, I. and Zhang, L. (2015), "Biopolymer stabilization of mine tailings for dust control", *J. Geotech. Geoenviron. Eng.*, **141**(2), 04014100. https://doi.org/10.1061/(ASCE)GT.1943-5606.0001240.

Fatehi, H., Ong, D.E. L., Yu, J. and Chang, I. (2021), "Biopolymers as green binders for soil improvement in geotechnical applications: A review", *Geosciences*, **11**(7). https://doi.org/10.3390/geosciences11070291.

Fatehi, H., Ong, D.E.L., Yu, J. and Chang, I. (2023), "The effects of particle size distribution and moisture variation on mechanical strength of biopolymer-treated soil", *Polymers*, **15**(6), 1549. https://doi.org/10.3390/polym15061549.

Garver, F., Sharma, M. and Pope, G. (1989), "The competition for chromium between xanthan biopolymer and resident clays in sandstones", SPE Annual Technical Conference and Exhibition.

Judge, P.K., Sundberg, E., DeGroot, D.J. and Zhang, G. (2022), "Effects of biopolymers on the liquid limit and undrained shear strength of soft clays", *Bull. Eng. Geol. Environ.*, **81**(8), 342. https://doi.org/10.1007/s10064-022-02830-9.

Kang, W., Ko, D. and Kang, J. (2021), "Erosion resistance performance of surface-reinforced levees using novel biopolymers investigated via real-scale overtopping experiments", *Water*, **13**(18), 2482. https://doi.org/10.3390/w13182482.

Kwon, Y.M., Ham, S.M., Kwon, T.H., Cho, G.C. and Chang, I. (2020), "Surface-erosion behaviour of biopolymer-treated soils assessed by EFA", *Géotechnique Lett.*, **10**(2), 106-112. https://doi.org/10.1680/jgele.19.00106.

Kwon, Y.M., Moon, J.H., Cho, G.C., Kim, Y.U. and Chang, I. (2023), "Xanthan gum biopolymer-based soil treatment as a construction material to mitigate internal erosion of earthen embankment: A field-scale", *Constr. Build. Mater.*, **389**, 131716. https://doi.org/10.1016/j.conbuildmat.2023.131716.

Latifi, N., Horpibulsuk, S., Meehan, C.L., Abd Majid, M.Z., Tahir, M.M. and Mohamad, E.T. (2017), "Improvement of problematic soils with biopolymer—an environmentally friendly soil stabilizer", *J. Mater. Civil Eng.*, **29**(2), 04016204. https://doi.org/10.1061/(ASCE)MT.1943-5533.0001706.

Lee, M., Chang, I., Kang, S.J., Lee, D.H. and Cho, G.C. (2023a), "Alkaline induced-cation crosslinking biopolymer soil treatment and field implementation for slope surface protection", *Geomech. Eng.*, **33**(1), 29-40. https://doi.org/10.12989/gae.2023.33.1.029.

Lee, M., Chang, I., Park, D.Y. and Cho, G.C. (2023b), "Strengthening and permeability control in sand using Cr3+-crosslinked xanthan gum biopolymer treatment", *Transp. Geotech.*, **43**, 101122. https://doi.org/10.1016/j.trgeo.2023.101122.

Lee, M., Chang, I.L. and Cho, G.C. (2023c), "Advanced biopolymer-based soil strengthening binder with trivalent chromium-xanthan gum crosslinking for wet strength and durability enhancement", *J. Mater. Civil Eng.*, **35**(10), 04023360. https://doi.org/10.1061/JMCEE7.MTENG-16123.

Lee, M., Im, J., Cho, G.C., Ryu, H.H. and Chang, I. (2020), "Interfacial shearing behavior along Xanthan gum biopolymer-treated sand and solid interfaces and its meaning in geotechnical engineering aspects", *Appl. Sci.*, **11**(1). https://doi.org/10.3390/app11010139.

Lee, M., Kwon, Y.M., Park, D.Y., Chang, I. and Cho, G.C. (2022), "Durability and strength degradation of xanthan gum based biopolymer treated soil subjected to severe weathering cycles", *Sci Rep.*, **12**(1), 19453. https://doi.org/10.1038/s41598-022-23823-4.

Lee, S., Chang, I., Chung, M.K., Kim, Y. and Kee, J. (2017), "Geotechnical shear behavior of Xanthan Gum biopolymer treated sand from direct shear testing", *Geomech. Eng.*, **12**(5), 831-847. https://doi.org/10.12989/gae.2017.12.5.831.

Lu, Z., Qiu, Y., Liu, J., Yu, C. and Yao, H. (2023), "Experimental study on microbially induced calcite precipitation for expansive soil stabilization", *Geomech. Eng.*, **32**(1), 85-96. https://doi.org/10.12989/gae.2023.32.1.085.

Ma, X., Zhao, C. and Zhu, J. (2021), "Aggravated risk of soil erosion with global warming–A global meta-analysis", *Catena*, **200**, 105129. https://doi.org/10.1016/j.catena.2020.105129.

Muguda, S., Booth, S.J., Hughes, P.N., Augarde, C.E., Perlot, C., Bruno, A.W. and Gallipoli, D. (2017), "Mechanical properties of biopolymer-stabilised soil-based construction materials", *Géotechnique Lett.*, **7**(4), 309-314.

Nugent, R.A. (2011), *The effect of exopolymers on the compressibility and shear strength of kaolinite*, Louisiana State University and Agricultural & Mechanical College.

Pelletier, E., Viebke, C., Meadows, J. and Williams, P.A. (2001), "A rheological study of the order-disorder conformational transition of xanthan gum", *Biopolymers*, **59**(5), 339-346. https://doi.org/10.1002/10970282(20011015)59:5%3C339::AID-BIP1031%3E3.0.CO;2-A.

Peppas, N.A. (1986), *Hydrogels in medicine and pharmacy* (Vol. 1). CRC press Boca Raton, FL. https://doi.org/10.1201/9780429285097.

Pratama, G.B.S., Yasuhara, H., Kinoshita, N., Putra, H., Almajed, A., Fukugaichi, S. and Ihsani, Z.M. (2024), "Efficacy of soybean-derived crude extract in enzyme-induced carbonate precipitation as soil-improvement technique", *Int. J. Geo. Eng.*, **15**(1), 14. https://doi.org/10.1186/s40703-024-00204-6.

Qureshi, M.U., Chang, I. and Al-Sadarani, K. (2017), "Strength and durability characteristics of biopolymer-treated desert sand", *Geomech. Eng.*, **12**(5), 785-801. https://doi.org/10.12989/gae.2017.12.5.785.

Rochefort, W.E. and Middleman, S. (1987), "Rheology of xanthan gum - salt, temperature, and strain effects in oscillatory and steady shear experiments", *J. Rheol.*, **31**(4), 337-369. https://doi.org/10.1122/1.549953.

Seo, S., Lee, M., Im, J., Kwon, Y.M., Chung, M.K., Cho, G.C. and Chang, I. (2021), "Site application of biopolymer-based soil treatment (BPST) for slope surface protection: in-situ wet-spraying method and strengthening effect verification", *Constr. Build. Mater.*, 307. https://doi.org/10.1016/j.conbuildmat.2021.124983.

Soldo, A. and Miletic, M. (2022), "Durability against wetting-drying cycles of sustainable biopolymer-treated soil", *Polymers*, **14**(19), 4247. https://doi.org/10.3390/polym14194247.

Soldo, A. and Miletić, M. (2019), "Study on shear strength of xanthan gum-amended soil", *Sustainability*, **11**(21), 6142. https://doi.org/10.3390/su11216142.

Tran, T.P.A., Cho, G.C. and Ilhan, C. (2020), "Water retention characteristics of biopolymer hydrogel containing sandy soils", *Hue Univ. J. Sci. Earth Sci. Environ.*, **129**(4). https://doi.org/10.26459/hueuni-jese.v129i4A.5652.

Vydehi, K.V., Moghal, A.A.B. and Basha, B.M. (2022), "Target reliability-based design of embankments using biopolymer-

modified cohesive soil", *Int. J. Geomech.*, **22**(8), 04022115. https://doi.org/10.1061/(ASCE)GM.1943-5622.0002429.